



# Inhibitory effect of berberine hydrochloride against *Candida albicans* and the role of the HOG-MAPK pathway

Xiaoxue Huang<sup>1,2</sup> · Yuling Yi<sup>3</sup> · Jiangyan Yong<sup>4</sup> · Jiayi Sun<sup>5</sup> · Zhen Song<sup>1</sup> · Dongmei Li<sup>1</sup> · Yan Li<sup>1</sup>

Received: 1 April 2021 / Revised: 23 June 2021 / Accepted: 26 July 2021 / Published online: 19 August 2021  
© The Author(s), under exclusive licence to the Japan Antibiotics Research Association 2021

## Abstract

Berberine hydrochloride (BH), an active component of *Coptis chinensis* and other plant taxa, has broad antimicrobial activity and may be useful for the treatment of *Candida* infections. In this study, the mechanisms underlying the inhibitory effect of BH against *Candida albicans* were evaluated, with a focus on the high-osmolarity glycerol mitogen-activated protein kinase (HOG-MAPK) pathway, which regulates multiple physiological functions. BH (256 and 64  $\mu\text{g ml}^{-1}$ ) significantly increased intracellular glycerol and ROS levels in *C. albicans*, inhibited germ tube and hyphal formation, and increased chitin and  $\beta$ -1,3-glucan exposure on the cell wall. The inhibitory effect of BH was positively correlated with its concentration, and the inhibitory effect of 256  $\mu\text{g ml}^{-1}$  BH was greater than that of 4  $\mu\text{g ml}^{-1}$  fluconazole (FLC). Furthermore, RT-PCR analysis showed that 256 and 64  $\mu\text{g ml}^{-1}$  BH altered the HOG-MAPK pathway in *C. albicans*. In particular, the upregulation of the core genes, *SLN1*, *SSK2*, *HOG1*, and *PBS2* may affect the expression of key downstream factors related to glycerol synthesis and osmotic pressure (*GPD1*), ROS accumulation (*ATP11* and *SOD2*), germ tube and hyphal formation (*HWPI*), and cell wall integrity (*CHS3* and *GSCI*). BH affects multiple biological processes in *C. albicans*; thus, it can be an effective alternative to conventional azole antifungal agents.

## Introduction

*Candida albicans* is a common fungal pathogen in humans that has been the focus of several clinical studies owing to the high mortality rate (up to 45%) of the invasive fungal

infection it causes [1]. However, owing to increasing drug resistance and the limited availability of agents that can be used in the treatment of the infections it causes, new antifungal drugs are urgently needed. Berberine is an isoquinoline alkaloid extracted from *Coptis chinensis*, which is a flowering plant belonging to the family Ranunculaceae and is native to China, particularly Sichuan. It can also be extracted from numerous other plant taxa, including *Berberis sargentiana* Schneid., *C. chinensis*, and *Phellodendron*, among which *C. chinensis* is its main source. It has anti-inflammatory, anti-oxidation, antiapoptotic, insulin resistance-promoting, and blood lipid level-lowering effects [2, 3]. Additionally, it shows antimicrobial activity against various bacterial taxa, including *Staphylococcus aureus*, *Escherichia coli*, *Pseudomonas aeruginosa*, and *C. albicans* [4]. However, the specific mechanism underlying its inhibitory effect against *C. albicans* is still unclear.

Sensing and responding to changes in the surrounding environment is essential for survival, and in fungi, the mitogen-activated protein kinase (MAPK) pathway mediates responses to a variety of stimuli. Specifically, the HOG-MAPK pathway, which has been extensively studied at the molecular level, is a classical MAPK pathway in *C. albicans* that participates in the regulation of many

**Supplementary information** The online version contains supplementary material available at <https://doi.org/10.1038/s41429-021-00463-w>.

✉ Yan Li  
Liliana@cduem.edu.cn

<sup>1</sup> College of Medical Technology, Chengdu University of Traditional Chinese Medicine, Chengdu, Sichuan, China

<sup>2</sup> West China School of Public Health and West China Fourth Hospital, Sichuan University, Chengdu, Sichuan, China

<sup>3</sup> The First People's Hospital of Chongqing Liang Jiang New Area, Chongqing, China

<sup>4</sup> Hospital of Chengdu University of Traditional Chinese Medicine, Chengdu, Sichuan, China

<sup>5</sup> Innovative Institute of Chinese Medicine and Pharmacy, Chengdu University of Traditional Chinese Medicine, Chengdu, Sichuan, China

important physiological functions. Osmotic pressure is sensed by a two-component sensor, Sln1, located in the plasma membrane of *C. albicans*. Under normal growth conditions, auto-phosphorylated Sln1 phosphorylates the response regulator Ssk1, resulting in its inactivation. Further, external osmotic pressure can inhibit the auto-phosphorylation of Sln1 and render Ssk1 non-phosphorylated, enabling it to bind to the N-terminal regulatory domain of Ssk2, leading to the phosphorylation and activation of Ssk2 [5], which is the only MAP3K in this pathway that is capable of regulating Hog1 via the activation of Pbs2 [6]. Further, Enjalbert et al. [7] identified *HOG1* as the core stress response gene in *C. albicans* via genome-wide transcriptional analysis. Therefore, it has been proposed that MAP3K (Ssk2) → MAP2K (Pbs2) → MAPK (Hog1) constitutes the central HOG-MAPK signaling pathway in *C. albicans* [8]. Furthermore, given that activated Hog1 is translocated into the nucleus, where it exerts regulatory effects depending on specific stimuli, the HOG-MAPK pathway may be involved in the regulation of intracellular osmotic pressure, oxidative stress pressure, respiratory metabolism, yeast-mycelium phase transition, and cell wall biosynthesis in *C. albicans* [9–15].

Studies have shown that the butyl alcohol extract of *Baitouweng* decoction increases the glycerol content in *C. albicans*, while octyl gallate and *Sanguinarine* inhibit the hyphal formation and *Paeonia lactiflora* inhibits cell wall synthesis [16–19]. Therefore, we hypothesized that berberine hydrochloride (BH) inhibits the growth of *C. albicans* via the HOG-MAPK pathway. To determine the mechanisms underlying the effects of BH on *C. albicans*, we analyzed the intracellular glycerol content, reactive oxygen species (ROS) content, ATP content, morphological transformation, cell wall components, and the expression levels of key genes and proteins in the HOG pathway in *C. albicans* following BH treatment.

## Materials and methods

### Strains and media

*C. albicans* (ATCC10231) was purchased from the Guangdong Microbial Strain Preservation Center. The strain was preserved in Yeast Extract Glucose Agar (Hopebio, Qingdao, China) containing glycerol at  $-80^{\circ}\text{C}$ . This medium contains 10.0 g peptone, 20.0 g glucose, 5.0 g yeast extract, and 14.0 g agar in 1.0 l tap water. Before the experiment, the strain was cultured at  $35^{\circ}\text{C}$  and 160 rpm for 24 h and passaged twice. The fungal solution was then diluted with sterile physiological saline and counted using a Bovine Bauer counter. The concentration of the fungal solution was adjusted to  $2 \times 10^6$  CFU  $\text{ml}^{-1}$ .

### Antimicrobial agents

BH (Pfeiffer Biotechnology, Chengdu, China) and fluconazole (FLC) were each dissolved with dimethyl sulfoxide to obtain 25.6 and 12.8  $\text{mg ml}^{-1}$  solutions, respectively. The solutions were thereafter sterilized using a sterile filter and kept in the dark at  $4^{\circ}\text{C}$ .

### Broth microdilution assay

The minimum inhibitory concentration (MIC) values of BH and FLC on ATCC10231 were determined according to the microbroth dilution method recommended by the Clinical and Laboratory Standards Institute (CLSI) M27-A4 program [20]. Briefly, the concentration of the prepared fungal solution was adjusted to  $4 \times 10^3$  CFU  $\text{ml}^{-1}$  with RPMI 1640 (Gibco, Grand Island, NY, USA), and then the solutions were added to a 96-well plate (100  $\mu\text{l}$ /well) such that the final concentrations of the fungal solution, BH, and FLC were  $2 \times 10^3$  CFU  $\text{ml}^{-1}$ , 256–0.25  $\mu\text{g ml}^{-1}$ , and 128–0.125  $\mu\text{g ml}^{-1}$ , respectively. The 96-well plate was incubated at  $35^{\circ}\text{C}$  for 24 h, and absorbance was measured at 450 nm ( $A_{450\text{nm}}$ ) using a microplate reader (Molecular Devices SpectraMax iD5, Shanghai, China); the lowest drug concentration required for the inhibition of the growth of 80% of *C. albicans* in the fungal solution was determined as the MIC. Blank controls were prepared without yeast, and drug-free wells were set as growth controls.

### Intracellular glycerol content assay

The effect of BH on the intracellular glycerol content of *C. albicans* was measured according to the method described by Hu et al [16], with some modifications. After the concentration of the fungal solution was adjusted to  $1 \times 10^6$  CFU  $\text{ml}^{-1}$  with RPMI 1640, the drugs were each added and the solutions were cultured at  $35^{\circ}\text{C}$  and 160 rpm for 24 h. Further, an appropriate amount of cell lysate was added to the fungal solutions followed by even mixing, and after standing at  $70^{\circ}\text{C}$ , the lipase was heat-inactivated and the supernatant was obtained via centrifugation. In 96-well plates, the sample (10  $\mu\text{l}$ ) and detection solution (190  $\mu\text{l}$ ) (Apply Technologies, Beijing, China) were added to each well. After reaction at  $37^{\circ}\text{C}$  for 10 min, the  $A_{550}$  of each well was determined using a microplate reader. Standard curves were then plotted to calculate the glycerol content of each sample fungal solution, which was thereafter corrected based on the number of cells per ml.

### Intracellular ROS assay

The effect of BH on intracellular ROS levels in *C. albicans* was evaluated as described previously [21, 22]. After drug treatment, the fungal solution was rinsed with sterile

phosphate-buffered saline (PBS), and its concentration was adjusted to  $2 \times 10^6$  CFU ml<sup>-1</sup> followed by the addition of DCFH-DA ( $20 \mu\text{g ml}^{-1}$ ; MeilunBio, Dalian, China) and the incubation of the samples for 40 min at 37 °C and 160 rpm. ROS levels in *C. albicans* were observed by dropping 10  $\mu\text{l}$  samples onto glass slides for observation under an inverted fluorescence microscope (OLYMPUS CKX53, Tokyo, Japan). After the reaction, the fungal solution was added to the 96-well plate, and the fluorescence intensity of each well was measured using a microplate reader (ex: 485 nm, em: 535 nm).

### Intracellular ATP content assay

The effect of BH on intracellular ATP content in *C. albicans* was evaluated according to the method described by Özdemir et al. [23]. The fungal solution obtained after drug treatment was collected and rinsed with sterile PBS, and its concentration was adjusted to  $1 \times 10^7$  CFU ml<sup>-1</sup>. Thereafter, *C. albicans* cells were lysed on ice and the supernatant was collected via centrifugation followed by the addition of the working enzyme solution (100  $\mu\text{l/well}$ ; Nanjing JianCheng, Nanjing, China) to a 96-well plate. After 1 min, the relative light unit value (RLU) of each well was determined. The standard curve was drawn by plotting the concentration of the standard against the RLU values corresponding to the different wells. This was followed by the calculation of the ATP content in each sample.

### Hyphal growth assay

According to a previously described protocol, a hyphal growth assay was performed, with slight modifications [24]. Briefly, the fungal solution ( $2 \times 10^6$  CFU ml<sup>-1</sup>) was added to the 96-well plate, treated as described in Table 1, and cultured at 35 °C for 4 and 6 h. Then, Hoechst33258 (Solarbio, Beijing, China) staining was used to observe the formation of hyphae under an inverted fluorescence microscope.

### Germ tube formation assay

The effect of BH on germ tube formation of *C. albicans* was evaluated as previously described by Zhao et al [25].

Specifically, RPMI 1640 medium containing 10% fetal bovine serum was used to adjust the concentration of the fungal solution to  $1 \times 10^6$  CFU ml<sup>-1</sup>. After drug treatment (Table 1), the culture was shaken at 35 °C and 160 rpm for 4 and 6 h. Then, 10  $\mu\text{l}$  of the fungal solution was added to the bovine Bauer counting board, and the number of germ tubes in 100 *C. albicans* cells was counted in random fields under a high-power microscope (OLYMPUS 4J0205, Tokyo, Japan). The rate of germ tube formation was then calculated as follows: Germ tube formation rate (%) = (number of germ tubes/number of *C. albicans*)  $\times$  100.

### Cell wall chitin exposure assay

To evaluate the effect of BH on the cell wall of *C. albicans*, a chitin exposure assay was performed [26]. After drug treatment, the fungal solution was rinsed with sterile PBS, and its concentration was adjusted to  $1 \times 10^7$  CFU ml<sup>-1</sup>, followed by the staining of the cells with calcium fluorescent white (GenMed Scientifics, Wilmington, DR, USA). Thereafter, 10  $\mu\text{l}$  of the fungal solution was dripped onto the glass slide and chitin exposure in the cell wall was observed via confocal laser scanning microscopy (CLSM) (ex: 405 nm, 630 $\times$ ) (LEICA TCS SP8 SR, Germany). The stained fungal solution (100  $\mu\text{l/well}$ ) was added to a 96-well plate, and the fluorescence intensity of each well was measured using a microplate reader (ex: 355 nm, em: 440 nm).

### Cell wall $\beta$ -1,3-glucan exposure assay

After drug treatment, the  $\beta$ -1,3-glucan content of *C. albicans* cell wall was determined [27]. Drug treatment and the collection of fungal fluid ( $2 \times 10^6$  CFU ml<sup>-1</sup>) were performed as previously described. Specifically, aniline blue (Solarbio) at a concentration of 0.1% was added to the fungal solution, followed by incubation at 80 °C for 15 min. After cooling to 25 °C, the dyed fungal solution (200  $\mu\text{l/well}$ ) was added to a 96-well plate and the fluorescence intensity of each well was measured using a microplate reader (ex: 398 nm, em: 508 nm).

**Table 1** Summary of the effects of berberine hydrochloride at various concentrations

Group	Glycerol content ( $\mu\text{mol ml}^{-1}$ )	ROS level	ATP content ( $\text{nmol l}^{-1}$ )	Chitin level	$\beta$ -1,3-glucan level
C	75.17 $\pm$ 3.26	142.13 $\pm$ 3.67	170 $\pm$ 4.53	2102.83 $\pm$ 9.48	316.07 $\pm$ 3.59
F	480.75 $\pm$ 4.55 $\blacklozenge$ $\blacktriangle$	1343.44 $\pm$ 29.23 $\blacklozenge$ $\blacktriangle$	617 $\pm$ 19.69 $\blacklozenge$ $\blacktriangle$	6012.63 $\pm$ 50.04 $\blacklozenge$ $\blacktriangle$	391.71 $\pm$ 12.88 $\blacklozenge$ $\blacktriangle$
A1	649.33 $\pm$ 9.42 $\blacklozenge$ $*$	462.875 $\pm$ 13.24 $\blacklozenge$ $*$	297 $\pm$ 12.54 $\blacklozenge$ $*$	16550.58 $\pm$ 75.07 $\blacklozenge$ $*$	2138.23 $\pm$ 7.92 $\blacklozenge$ $*$
A2	144.08 $\pm$ 5.88 $\blacklozenge$ $\blacktriangle$ $*$	187.02 $\pm$ 4.28 $\blacklozenge$ $\blacktriangle$ $*$	234 $\pm$ 8.56 $\blacklozenge$ $\blacktriangle$ $*$	2705.60 $\pm$ 11.33 $\blacklozenge$ $\blacktriangle$ $*$	412.88 $\pm$ 13.97 $\blacklozenge$ $\blacktriangle$ $*$
A3	103.75 $\pm$ 5.95 $\blacklozenge$ $\blacktriangle$ $*$	165.32 $\pm$ 5.27 $\blacklozenge$ $\blacktriangle$ $*$	210 $\pm$ 11.42 $\blacklozenge$ $\blacktriangle$ $*$	2162.64 $\pm$ 17.45 $\blacklozenge$ $\blacktriangle$ $*$	331.05 $\pm$ 5.54 $\blacklozenge$ $\blacktriangle$ $*$

$\blacklozenge$  compared with the negative control group,  $P < 0.05$ ;  $\blacktriangle$  compared with the 256  $\mu\text{g ml}^{-1}$  BH group,  $P < 0.05$ ;  $*$  compared with 4  $\mu\text{g ml}^{-1}$  FLC group,  $P < 0.05$

C blank control; F: 4  $\mu\text{g ml}^{-1}$  FLC; A1: 256  $\mu\text{g ml}^{-1}$  BH; A2: 64  $\mu\text{g ml}^{-1}$  BH; A3: 16  $\mu\text{g ml}^{-1}$  BH

## Quantitative reverse transcription PCR

To explore the effect of BH on the HOG-MAPK pathway, quantitative reverse transcription PCR (qRT-PCR) was performed [28]. After adjusting the concentration of the prepared *C. albicans* solution to  $1 \times 10^6$  CFU ml<sup>-1</sup> with RPMI 1640, the corresponding drugs were added followed by the shaking of the resulting solutions for 24 h at 35 °C and 160 rpm. The cells were then washed and total RNA was extracted using TRIzol reagent (Invitrogen, Carlsbad, CA, USA). TransScript First-Strand cDNA Synthesis SuperMix (TransGen, Beijing, China) was used to synthesize cDNA for qPCR. Primers for target genes and the internal reference gene (*ACT1*) were designed and synthesized by Shanghai Shengong Bioengineering Co., Ltd. (Supplementary Table 1). The qPCR system was composed of cDNA (20 µl), primers, and TransStart Green qPCR SuperMix (TransGen), and the qRT-PCR was performed using the qTower Real-time PCR System (Analytik Jena qtower2.2, Germany) as follows: pre-denaturation at 94 °C, denaturation at 94 °C, denaturation at 57 °C, annealing at 57 °C, and extension for 10 s at 72 °C, for a total of 40 cycles. The melting curve was analyzed at temperatures in the range 60–95 °C. Relative target gene expression fold changes were calculated using the  $2^{-\Delta\Delta ct}$  method.

## Western blotting

The effect of BH on Hog1 was analyzed according to the methods described by Mancuso et al. [29], with some modifications. The fungal solution was treated and collected according to the method described for total protein extraction. The Protein Extraction Kit (Keygen, Nanjing, China) was used to extract total protein, and the protein concentration was determined using the BCA Protein Quantitative Kit (Beyotime, Beijing, China). The prepared protein sample was then separated using SDS-PAGE and transferred to a PVDF membrane. The membrane containing Hog1 was then incubated with the appropriate antibody (Supplementary Table 2), and a gel imager (Analytik Jena UVP Chemstudio, Germany) was used to obtain images. The gray values of each strip were analyzed using ImageJ (NIH, Bethesda, MD, USA), and the results were expressed as the ratio of the gray value corresponding to the target protein, Hog1, to the gray value corresponding to the reference protein,  $\beta$ -tubulin, in the corresponding channel.

## Statistical Analysis

SPSS Statistics v21.0 was used to analyze differences among experimental groups via ANOVA, and the results obtained were presented as  $\bar{x} \pm S$ .  $P < 0.05$  was considered statistically significant. All the experiments were performed in triplicates on different days.

## Results

### MIC of BH and FLC and optimization of drug concentrations

BH showed good antifungal activity against ATCC10231 with a MIC of 64 µg ml<sup>-1</sup>. In further analyses, BH at 4 × MIC, MIC, and ¼ × MIC (i.e., 256, 64, and 16 µg ml<sup>-1</sup>, respectively) were evaluated in comparison with FLC (4 × MIC; 4 µg ml<sup>-1</sup>), which currently is one of the most effective drug for the treatment of infections caused by *C. albicans*, as a positive drug control.

### BH increases the intracellular osmotic pressure

The intracellular glycerol contents of *C. albicans* were higher in the 256, 64, and 16 µg ml<sup>-1</sup> BH-treatment groups than in the control group ( $P < 0.05$ ). Further, in the BH-treatment groups, the variation of the intracellular glycerol contents followed the order: 256 µg ml<sup>-1</sup> BH > 64 µg ml<sup>-1</sup> BH > 16 µg ml<sup>-1</sup> BH ( $P < 0.05$ ), and treatment with 256 µg ml<sup>-1</sup> BH resulted in a higher intracellular glycerol content than treatment with 4 µg ml<sup>-1</sup> FLC ( $P < 0.05$ ) (Table 1).

### BH increases ROS levels in ATP contents in cells

Intracellular ROS levels and ATP contents were higher in the 256, 64, and 16 µg ml<sup>-1</sup> BH treatment groups than in the blank control group ( $P < 0.05$ ). Further, considering the BH treatment groups only, intracellular ROS levels and ATP contents varied in the order: 256 µg ml<sup>-1</sup> BH > 64 µg ml<sup>-1</sup> BH > 16 µg ml<sup>-1</sup> BH ( $P < 0.05$ ). However, the ROS levels and ATP contents resulting from treatment with 4 µg ml<sup>-1</sup> FLC were higher than those corresponding to all the other treatment groups ( $P < 0.05$ ) (Table 1). Consistent with these results, the DCFH-DA fluorescence intensity in ATCC10231 cells, as determined under an inverted microscope, decreased in the following order: 4 µg ml<sup>-1</sup> FLC > 256 µg ml<sup>-1</sup> BH > 64 µg ml<sup>-1</sup> BH > 16 µg ml<sup>-1</sup> BH > blank control (Fig. 1).

### BH inhibits hyphal and germ tube formation

After 4 h of drug intervention, the 256 µg ml<sup>-1</sup> BH group mainly included yeast phase cells and the cell count decreased. Cells in the 64 µg ml<sup>-1</sup> BH group formed shorter hyphae, while cells in the 16 µg ml<sup>-1</sup> BH group and the control group formed long hyphae that were interwoven. The 4 µg ml<sup>-1</sup> FLC group mainly formed short germ tubes. At 6 h after drug intervention, the formation of hyphae in each group was consistent with that at 4 h; however, the number of cells was relatively higher and the hyphae were longer (Fig. 2a).

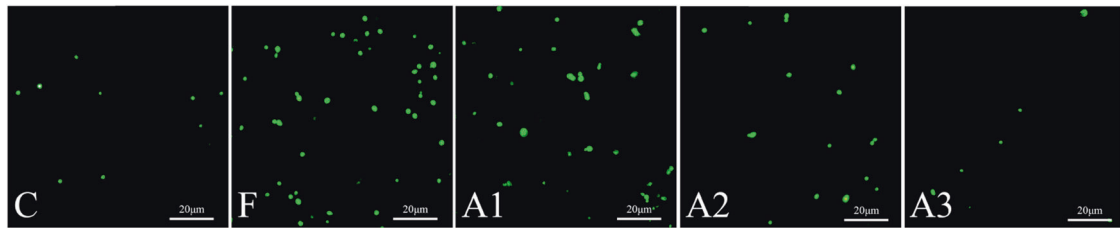
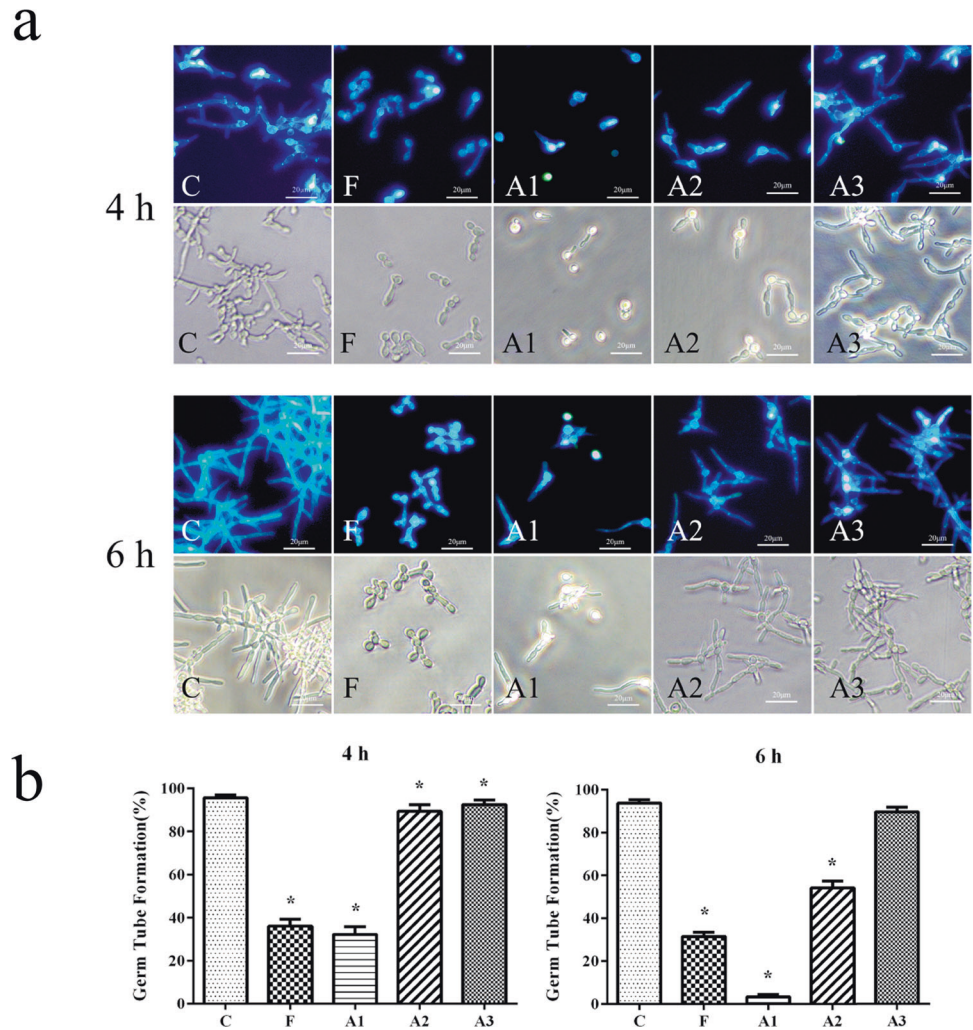


**Fig. 1** ROS levels in ATCC 10231 after drug intervention (fluorescent Inverted microscope, 200 $\times$ ). ROS in *C. albicans* cells reacted with DCFH-DA fluorescent probe and emitted green fluorescence under excitation. C, blank control; F, 4  $\mu\text{g ml}^{-1}$  FLC; A1, 256  $\mu\text{g ml}^{-1}$  BH; A2, 64  $\mu\text{g ml}^{-1}$  BH; and A3, 16  $\mu\text{g ml}^{-1}$  BH.

**Fig. 2 a** Hyphae and **b** Germ tube formation in ATCC 10231 after 4 h and 6 h of drug intervention. Hyphae were stained using Hoechst 33258 and observed under an inverted fluorescent microscope (200 $\times$ ), while the number of germ tubes in 100 *C. albicans* cells were counted in random fields under a high-power microscope and the germ tube formation rate was calculated. \* compared with the negative control group,  $P < 0.05$ ; C blank control; F, 4  $\mu\text{g ml}^{-1}$  FLC; A1, 256  $\mu\text{g ml}^{-1}$  BH; A2, 64  $\mu\text{g ml}^{-1}$  BH; and A3, 16  $\mu\text{g ml}^{-1}$  BH



After 4 h of drug intervention, the germ tube formation rates corresponding to the BH treatments, which were all lower than that corresponding to the control group ( $P < 0.05$ ), varied in the order: 256  $\mu\text{g ml}^{-1}$  BH < 64  $\mu\text{g ml}^{-1}$  BH < 16  $\mu\text{g ml}^{-1}$  BH ( $P < 0.05$ ). It was also observed that the germ tube formation rate observed following the 256  $\mu\text{g ml}^{-1}$  BH treatment was lower than that resulting from the 4  $\mu\text{g ml}^{-1}$  FLC treatment ( $P < 0.05$ ), and after 6 h of treatment, the rates of germ tube formation in the 256 and 64  $\mu\text{g ml}^{-1}$  BH groups were similar to

those at 4 h, and those corresponding to the 16  $\mu\text{g ml}^{-1}$  BH and control groups showed no significant difference ( $P > 0.05$ ) (Fig. 2b).

### BH increases cell wall chitin and $\beta$ -1,3-glucan contents

The cell volume of *C. albicans* in the 256  $\mu\text{g ml}^{-1}$  BH group was significantly increased and fluorescence intensity

**Fig. 3** Chitin exposure in the ATCC 10231 cell wall after drug intervention (CLSM, 630 $\times$ ). *C. albicans* cells were stained with calcium fluorescent white (CFW) and the chitin exposed in the cell wall was stained. Its emission of blue light was then monitored. C blank control; F, 4  $\mu\text{g ml}^{-1}$  FLC; A1, 256  $\mu\text{g ml}^{-1}$  BH; A2, 64  $\mu\text{g ml}^{-1}$  BH; and A3, 16  $\mu\text{g ml}^{-1}$  BH

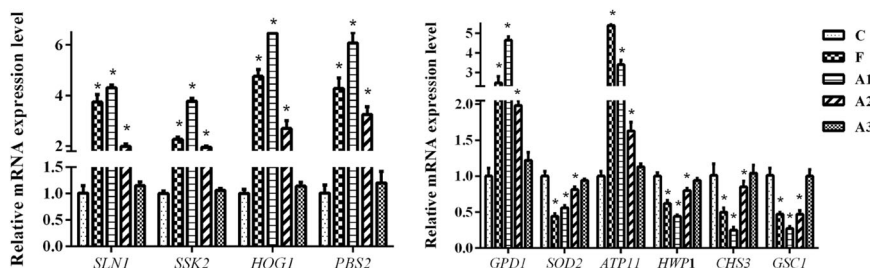
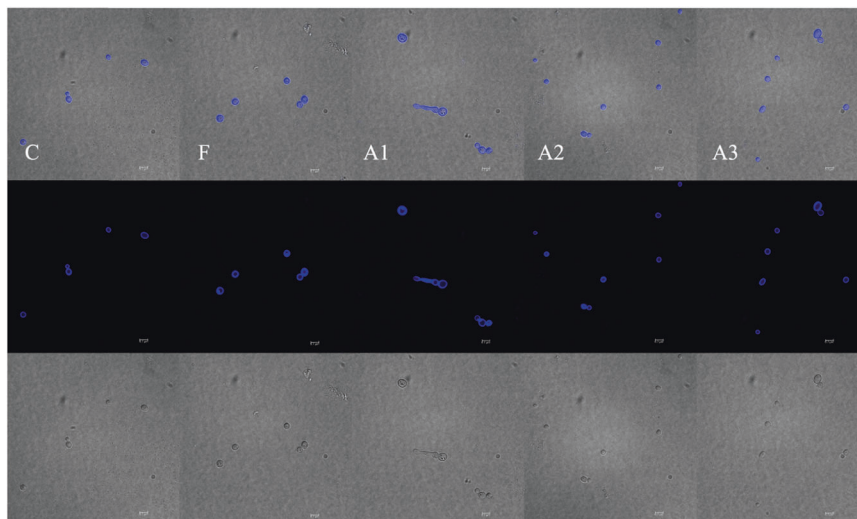


**Fig. 4** Gene expression in ATCC 10231 after BH treatment. *C. albicans* cells were treated with BH at 35  $^{\circ}\text{C}$  for 24 h and then collected for RNA extraction. \* compared with the negative control group,  $P < 0.05$ ; C

blank control; F, 4  $\mu\text{g ml}^{-1}$  FLC; A1, 256  $\mu\text{g ml}^{-1}$  BH; A2, 64  $\mu\text{g ml}^{-1}$  BH; and A3, 16  $\mu\text{g ml}^{-1}$  BH

was the highest. The cell volume of the 4  $\mu\text{g ml}^{-1}$  FLC group was normal but the fluorescence intensity for the chitin marker was significantly higher than that of the other three groups. The cells in the 64 and 16  $\mu\text{g ml}^{-1}$  BH groups and blank control were normal, while fluorescence intensity was higher in the 64  $\mu\text{g ml}^{-1}$  BH group than in the other groups (Fig. 3).

Levels of cell wall chitin were consistent with results obtained by CLSM. Levels of chitin and  $\beta$ -1,3-glucan in the cell wall were higher in the 256 and 64  $\mu\text{g ml}^{-1}$  BH groups than in the control group ( $P < 0.05$ ); however, there was no significant difference in chitin level between the 16  $\mu\text{g ml}^{-1}$  BH and control groups ( $P > 0.05$ ) while it was opposite in  $\beta$ -1,3-glucan level ( $P < 0.05$ ). Further, the variation of cell wall chitin and  $\beta$ -1,3-glucan levels followed the order: 256  $\mu\text{g ml}^{-1}$  BH > 64  $\mu\text{g ml}^{-1}$  BH > 16  $\mu\text{g ml}^{-1}$  BH ( $P < 0.05$ ). Additionally, 256 and 64  $\mu\text{g ml}^{-1}$  BH treatments resulted in higher cell wall  $\beta$ -1,3-glucan levels than in the 4  $\mu\text{g ml}^{-1}$  FLC treatment; while only the 256  $\mu\text{g ml}^{-1}$  BH-treated group showed higher chitin levels than the FLC group ( $P < 0.05$ ) (Table 1).

### BH induces the expression of multiple genes

The effects of BH on the HOG-MAPK pathway and the downstream genes in *C. albicans* were detected via qRT-PCR (Fig. 4). BH (256 and 64  $\mu\text{g ml}^{-1}$ ) significantly upregulated the expression of key nodes in the HOG pathway, i.e., *SLN1*, *SSK2*, *HOG1*, and *PBS2* (all  $P < 0.05$ ), with no differences between the 16  $\mu\text{g ml}^{-1}$  BH and control groups ( $P > 0.05$ ). Expression levels of these genes were higher in the 256  $\mu\text{g ml}^{-1}$  BH group than in the 4  $\mu\text{g ml}^{-1}$  FLC group ( $P < 0.05$ ).

*GPD1* and *ATP11* levels were significantly higher in the 256 and 64  $\mu\text{g ml}^{-1}$  BH groups than in the control group ( $P < 0.05$ ) but did not differ significantly between the 16  $\mu\text{g ml}^{-1}$  BH group and the control group ( $P > 0.05$ ). Compared with levels in the 4  $\mu\text{g ml}^{-1}$  FLC group, *GPD1* expression was higher and *ATP11* was lower in the 256  $\mu\text{g ml}^{-1}$  BH group ( $P < 0.05$ ). Compared with levels in the control group, *SOD2*, *HWPI*, *CHS3*, and *GSCI* levels were significantly lower in the 256 and 64  $\mu\text{g ml}^{-1}$  BH groups ( $P < 0.05$ ), with no difference

in the  $16 \mu\text{g ml}^{-1}$  BH group ( $P > 0.05$ ). Compared with levels in the  $4 \mu\text{g ml}^{-1}$  FLC group, *SOD2* levels were higher and *HWP1*, *CHS3*, and *GSC1* levels were lower in the  $256 \mu\text{g ml}^{-1}$  BH group ( $P < 0.05$ ). There was no significant difference in *GSC1* expression between the  $64 \mu\text{g ml}^{-1}$  BH and  $4 \mu\text{g ml}^{-1}$  FLC groups, but the expression of other genes was significantly higher in the  $64 \mu\text{g ml}^{-1}$  BH group ( $P < 0.05$ ). These results indicated that BH upregulates *GPD1* and *ATP11*, key downstream genes of the HOG pathway, and inhibits *SOD2*, *HWP1*, *CHS3*, and *GSC1*.

### BH upregulates Hog1 protein expression

Compared with levels in the control group, Hog1 protein levels in the  $256 \mu\text{g ml}^{-1}$  BH group were significantly higher ( $P < 0.05$ ). Further, Hog1 was slightly upregulated in the  $64$  and  $16 \mu\text{g ml}^{-1}$  BH groups, but the differences were not statistically significant ( $P > 0.05$ ). Compared with levels in the  $4 \mu\text{g ml}^{-1}$  FLC group, Hog1 protein levels in the  $64$  and  $16 \mu\text{g ml}^{-1}$  BH groups were lower ( $P < 0.05$ ), with no difference in the  $256 \mu\text{g ml}^{-1}$  BH group ( $P > 0.05$ ) (Fig. 5).

### Discussion

The HOG-MAPK pathway affects *C. albicans* growth by regulating its adaptation to external osmotic and oxidative pressure, morphological transformation, and cell wall synthesis. Further, the *C. albicans* HOG-MAPK central signaling pathway, MAP3K (Ssk2)  $\rightarrow$  MAP2K (Pbs2)  $\rightarrow$  MAPK (Hog1), has an upstream regulatory role in these processes. We found BH at  $256$  and  $64 \mu\text{g ml}^{-1}$  significantly upregulated *SLN1*, *SSK2*, *PBS2*, and *HOG1* in *C. albicans*, suggesting that the inhibitory effect of BH on *C. albicans* may be related to the upregulation of these key node genes in the HOG-MAPK pathway. Additionally, only  $256 \mu\text{g ml}^{-1}$  BH increased Hog1 protein expression, whereas both  $256$  and  $64 \mu\text{g ml}^{-1}$  BH brought about an increase in *HOG1* mRNA expression. Possibly, this observation can be attributed to the fact that Hog1 is not a

complete constitutive protein, and its expression increases inductively when it is subjected to some stimulation [30, 31]. Further, it has been demonstrated that protein expression is affected by the regulation of mRNA stability, the effectiveness of mRNA translation, and the stability of the protein itself. These factors led to the inconsistency in the expression levels of the *HOG1* gene and Hog1 protein. Furthermore, high drug concentrations possibly have a more significant effect on Hog1 protein expression, which may be dose-dependent. Accordingly, to exert an effect on protein expression, high drug concentrations are needed.

Butyl alcohol extract of *Baitouweng* decoction has shown to increase the intracellular glycerol content, membrane permeability, and the degree of cell membrane damage in *C. albicans* in a dose-dependent manner [16]. Similarly, the results of this study showed that  $256$  and  $64 \mu\text{g ml}^{-1}$  BH significantly increased the intracellular glycerol content and intracellular osmotic pressure of *C. albicans*. Therefore, we speculated that BH damages the cell membrane integrity of *C. albicans*. Phosphorylated Hog1 enters the nucleus and binds to transcription factors to increase intracellular osmotic pressure and resist external hyperosmotic pressure by preventing intracellular glycerol efflux and increasing the glycerol content. Hyperosmotic stress can upregulate the expression of Hog1-dependent *GPD1*, *GPD2*, and other glycerol biosynthesis-related genes, while only *GPD1* is necessary for osmotic adaptation [32]. Our results suggested that  $256$  and  $64 \mu\text{g ml}^{-1}$  BH treatments increase the intracellular osmotic pressure in *C. albicans* via the upregulation of *GPD1* and the promotion of intracellular glycerol synthesis.

According to the chemiosmotic hypothesis, the mitochondrial membrane potential directly reflects respiratory chain activity, which is closely related to ATP production, and ROS production shows an exponential relationship with the mitochondrial membrane potential [33]. Octyl gallate ( $25 \mu\text{g ml}^{-1}$ ) can produce abundant ROS, resulting in membrane lipid peroxidation and membrane damage, thereby effectively inhibiting *C. albicans* [17]. We observed similar effects following treatment with  $256$  and  $64 \mu\text{g ml}^{-1}$  BH, which significantly increased intracellular ROS levels and ATP contents in *C. albicans*. ATP is mainly synthesized in mitochondria via ATP synthase complex (F0-F1 ATPase), and Atp11p, encoded by *ATP11*, is essential for the complex assembly [34, 35]. Endogenous ROS produced during aerobic respiration can effectively damage *C. albicans* cells, and intracellular ROS concentration depends on the balance between their production and clearance by various antioxidant compounds and enzymes. SOD, encoded by *SOD1/SOD2*, is the only known enzyme that scavenges free radicals directly and plays an important role in *C. albicans* [36]. We found that  $256$  and  $64 \mu\text{g ml}^{-1}$  BH increased *ATP11* expression and significantly inhibited *SOD2* expression, suggesting that BH

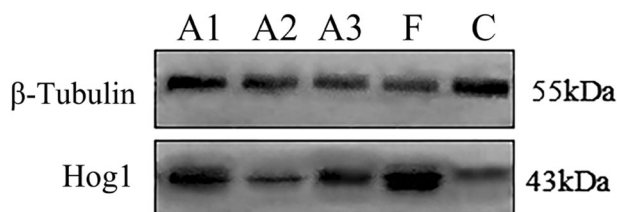


**Fig. 5** Hog1 protein expression in ATCC 10231 in response to BH intervention. *C. albicans* cells were treated with BH at  $35^\circ\text{C}$  for 24 h and collected for total protein extraction. C blank control; F,  $4 \mu\text{g ml}^{-1}$  FLC; A1,  $256 \mu\text{g ml}^{-1}$  BH; A2,  $64 \mu\text{g ml}^{-1}$  BH; and A3,  $16 \mu\text{g ml}^{-1}$  BH

enhances the aerobic respiratory metabolism of mitochondria and increases ROS production, while also causing intracellular ROS accumulation, cell damage, and cell death. FLC and miconazole can increase endogenous ROS levels in drug-sensitive fungi, suggesting that the increase in ROS levels is an antifungal mechanism of azole drugs [37]. This may explain why the effect of 256  $\mu\text{g ml}^{-1}$  BH on ROS levels was weaker than that of 4  $\mu\text{g ml}^{-1}$  FLC.

Hyphae play a critical role in the process of infection; they promote *C. albicans* invasion of human tissues and escape from immune cells [38]. Here, it was observed that BH can inhibit germ tube and hyphal formation in a dose-dependent manner, and 256  $\mu\text{g ml}^{-1}$  BH could maintain a good inhibitory effect with the extension of culture time, consistent with previous findings for *Sanguinarine* [18]. The hyphae-specific gene *HWPI* is highly upregulated during the growth of hyphae [39]. Lee et al. [40, 41] found that both nepodin and 6-gingerol could inhibit the hyphal formation of *C. albicans* via decreases in *HWPI* and *ECE1* expression, similar to our results for BH.

Fungal cell wall proteins and polysaccharides have good antigenicity; they can be recognized by innate immune cells, such as macrophages and neutrophils, in the human body and can act as intermediates of fungal–host interactions. Therefore, these proteins are good therapeutic drug targets [42, 43]. Our results showed that 256 and 64  $\mu\text{g ml}^{-1}$  BH could significantly increase  $\beta$ -1,3-glucan and chitin in the cell wall of *C. albicans*. Thus, BH may lead to *C. albicans* death by damaging the structural integrity of the cell wall and increasing the exposure of cell wall components. Similarly, it has also been observed that the ethanol extract of *P. lactiflora* inhibits *C. albicans*  $\beta$ -1,3-glucan synthetase and damages cell wall integrity [19]. We found that 256 and 64  $\mu\text{g ml}^{-1}$  BH could significantly inhibit the expression of *CHS3*, which is responsible for chitin short rod production [44], and *GSCI*, which regulates cell wall remodeling [45, 46] and  $\beta$ -1,3-glucan synthesis [47], in *C. albicans*. It was speculated that BH could downregulate genes encoding chitin synthase and  $\beta$ -1,3-glucan synthase in *C. albicans*, thereby damaging cell wall integrity. Our results corroborated previous findings; *FKS1* and *CHS3* levels in *C. albicans* are significantly downregulated by the butyl alcohol extract of *Baitouweng* decoction [16].

The effects of 256  $\mu\text{g ml}^{-1}$  BH on *C. albicans* were stronger than those of 4  $\mu\text{g ml}^{-1}$  FLC, a first-line clinical antifungal therapy. Azole antifungal agents inhibit the biosynthesis of ergosterol (essential for cell integrity and membrane function) by inactivating lanosterol 14  $\alpha$ -demethylase, leading to a decrease in ergosterol levels in the cell membrane and an increase in intermediate metabolites [48]. Unlike FLC, which has a single target, BH has multiple antimicrobial pathways and targets; this renders the development of drug resistance more difficult [49]. Although we evaluated the core genes in the

HOG-MAPK central signaling pathway and downstream effector genes, the interactions between these genes need to be studied further. In addition, owing to limitations associated with the availability of commercial reagents, the expression of other key proteins in the pathway were not investigated. Moreover, detecting the expression of phosphorylated Hog1 after drug intervention may reflect the effect of BH on the HOG-MAPK pathway more accurately. We will supplement this research in this regard in our future studies. Further, given that it has been demonstrated that the *HOG1* mutant strain of *C. albicans* is resistant to Congo red [15], while the mutant strain lacking *HOG1* is more susceptible to AMB than the wild type strain [50], it would be necessary to determine the effect of BH on the Hog1 $\Delta$  strain in future studies. Therefore, we will construct the Hog1 $\Delta$  strain through homologous recombination and Leu-His marker screening [51], considering this issue as one of the research objects in our future studies. These limitations will be addressed in follow-up studies to further improve our understanding of the therapeutic effects of BH. This study provides a reference for the application of BH to inhibit *C. albicans*, and contributes to the development of new antifungal agents and the clinical treatment of *C. albicans* infection.

Supplementary information is available at The Journal of Antibiotics website.

**Acknowledgements** This work was supported by the Health Commission of Sichuan Province, People's Republic of China (20PJ163), and the "Xinglin Scholar" Scientific Research Project of Chengdu University of TCM (JSZX2018006). We would like to thank Editage [[www.editage.cn](http://www.editage.cn)] for English language editing.

**Author contributions** X.H. and Y.L. conceived and designed the research. X.H. and Y.Y. performed most of the experiments. J.Y. and J.S. contributed to reagents, data analysis, and results in interpretation with the assistance of Z.S. and D.L. X.H. wrote the initial paper and Y.L. revised the paper. All authors approved the manuscript for publication.

## Compliance with ethical standards

**Conflict of interest** The authors declare no competing interests.

**Publisher's note** Springer Nature remains neutral with regard to jurisdictional claims in published maps and institutional affiliations.

## References

1. Rauseo AM, Coler-Reilly A, Larson L, Spec A. Hope on the horizon: novel fungal treatments in development. *Open Forum Infect Dis.* 2020;7:ofaa016.
2. Liu DQ, Chen SP, Sun J, Wang XM, Chen N, Zhou YQ, et al. Berberine protects against ischemia-reperfusion injury: a review of evidence from animal models and clinical studies. *Pharm Res.* 2019;148:104385.
3. Imenshahidi M, Hosseinzadeh H. Berberine and barberry (*Berberis vulgaris*): a clinical review. *Phytother Res.* 2019;33:504–23.
4. Tillhon M, Ortiz LMG, Lombardi P, Scovassi AI. Berberine: new perspectives for old remedies. *Biochem Pharmacol.* 2012;84:1260–7.



5. Horie T, Tatebayashi K, Yamada R, Saito H. Phosphorylated Ssk1 prevents unphosphorylated Ssk1 from activating the Ssk2 mitogen-activated protein kinase in the yeast high-osmolarity glycerol osmoregulatory pathway. *Mol Cell Biol.* 2008;28:5172–83.
6. Cheetham J, Smith DA, da Silva DA, Doris KS, Patterson MJ, Bruce CR, et al. A single MAPKKK regulates the Hog1 MAPK pathway in the pathogenic fungus *Candida albicans*. *Mol Biol Cell.* 2007;18:4603–14.
7. Enjalbert B, Smith DA, Cornell MJ, Alam I, Nicholls S, Brown AJP, et al. Role of the Hog1 stress-activated protein kinase in the global transcriptional response to stress in the fungal pathogen *Candida albicans*. *Mol Biol Cell.* 2006;17:1018–32.
8. Román E, Correia I, Prieto D, Alonso R, Pla J. The HOG MAPK pathway in *Candida albicans*: more than an osmosensing pathway. *Int Microbiol.* 2020;23:23–9.
9. Liu S, Chen C. Advances in MAPK signaling pathway in pathogenic fungi. *Hunan Agric Sci.* 2017;11:119–22.
10. Dunayevich P, Baltanás R, Clemente JA, Couto A, Sapochnik D, Vasen G, et al. Heat-stress triggers MAPK crosstalk to turn on the hyperosmotic response pathway. *Sci Rep.* 2018;8:15168.
11. Correia I, Alonso-Monge R, Pla J. The Hog1 MAP kinase promotes the recovery from cell cycle arrest induced by hydrogen peroxide in *Candida albicans*. *Front Microbiol.* 2017;6:2133.
12. Lee YM, Kim E, An J, Lee Y, Choi E, Choi W, et al. Dissection of the HOG pathway activated by hydrogen peroxide in *Saccharomyces cerevisiae*. *Environ Microbiol.* 2017;19:584–97.
13. Su C, Lu Y, Liu H. Reduced TOR signaling sustains hyphal development in *Candida albicans* by lowering Hog1 basal activity. *Mol Biol Cell.* 2013;24:385–97.
14. Alonso-Monge R, Carvaihlo S, Nombela C, Rial E, Pla J. The Hog1 MAP kinase controls respiratory metabolism in the fungal pathogen *Candida albicans*. *Microbiol.* 2009;155:413–23.
15. Morales-Menchén A, Navarro-García F, Guirao-Abad JP, Román E, Prieto D, Coman IV, et al. Non-canonical activities of Hog1 control sensitivity of *Candida albicans* to killer toxins from *Debaryomyces hansenii*. *Front Cell Infect Microbiol.* 2018;8:135.
16. Hu TL, Yun Y, Xu ZQ, Duan QJ, Shao J, Wang TM, et al. Butyl alcohol extract of *Zaitouweng* decoction inhibits *Candida albicans* cell membrane. *J Chin Mater Med.* 2017;42:3185–90.
17. Saibabu V, Fatima Z, Ahmad K, Khan LA, Hameed S. Octyl gallate triggers dysfunctional mitochondria leading to ROS driven membrane damage and metabolic inflexibility along with attenuated virulence in *Candida albicans*. *Med Mycol.* 2020;58:380–92.
18. Zhong H, Hu DD, Hu GH, Su J, Bi S, Zhang ZE, et al. Activity of Sanguinarine against *Candida albicans* biofilms. *Antimicrob Agents Chemother.* 2017;61:e02259–16.
19. Lee HS, Kim Y. *Paeonia lactiflora* inhibits cell wall synthesis and triggers membrane depolarization in *Candida albicans*. *J Microbiol Biotechnol.* 2017;27:395–404.
20. CLSI. Reference method for broth dilution antifungal susceptibility testing of yeasts. 4th ed. Wayne (PA): Clinical and Laboratory Standards Institute; 2017.
21. Ding T, Wang SF, Zhang XY, Zai WJ, Fan JJ, Chen W, et al. Kidney protection effects of dihydroquercetin on diabetic nephropathy through suppressing ROS and NLRP3 inflammation. *Phytomedicine.* 2018;41:45–53.
22. Afri M, Frimer AA, Cohen Y. Active oxygen chemistry within the liposomal bilayer. Part IV: locating 2',7'-dichlorofluorescein (DCF), 2',7'-dichlorodihydrofluorescein (DCFH) and 2',7'-dichlorodihydrofluorescein diacetate (DCFH-DA) in the lipid bilayer. *Chem Phys Lipids.* 2004;131:123–33.
23. Özdemir A, Altıntop MD, Sever B, Gençer HK, Kapkaç HA, Atlı O, et al. A new series of pyrrole-based chalcones: synthesis and evaluation of antimicrobial activity, cytotoxicity, and genotoxicity. *Molecules.* 2017;22:E2112.
24. Nakamura A, Takigawa K, Kurishita Y, Kuwata K, Ishida M, Shimoda Y, et al. Hoechst tagging: a modular strategy to design synthetic fluorescent probes for live-cell nucleus imaging. *Chem Commun.* 2014;50:6149–52.
25. Zhao XY, Guo G, Su PP, Yang LJ, Zhu LJ, Tian ZQ, et al. Inhibitory effect of housefly antimicrobial peptide AMP-17 on hyphae of *Candida albicans*. *Microbiol China.* 2017;12:1–15.
26. Li Y, Sun H, Zhu X, Bian C, Wang YC, Si S. Identification of new antifungal agents targeting chitin synthesis by a chemical-genetic method. *Molecules.* 2019;24:E3155.
27. Liu YF, Tang QJ, Zhang JS, Zhou S, Wang CG, Yang Y, et al. Determination of  $\beta$ -1,3-glucan content and analysis of polysaccharide composition from *Ganoderma lingzhi* extract. *Mycosystema.* 2018;37:1525–31.
28. Haque F, Alfatah M, Ganesan K, Bhattacharyya MS. Inhibitory effect of sophorolipid on *Candida albicans* biofilm formation and hyphal Growth. *Sci Rep.* 2016;6:23575.
29. Mancuso R, Chinnici J, Tsou C, Busarajan S, Munnangi R, Maddi A. Functions of *Candida albicans* cell wall glycosidases Dfg5p and Dcw1p in biofilm formation and HOG MAPK pathway. *PeerJ.* 2018;6:e5685.
30. Guerra-Moreno A, Ang J, Welsch H, Jochem M, Hanna J. Regulation of the unfolded protein response in yeast by oxidative stress. *FEBS Lett.* 2019;593:1080–88.
31. Liu NN, Uppulur P, Broggi A, Besold A, Ryman K, Kambara H, et al. Intersection of phosphate transport, oxidative stress and TOR signalling in *Candida albicans* virulence. *PLoS Pathog.* 2018;14:e1007076.
32. Hohmann S. An integrated view on a eukaryotic osmoregulation system. *Curr Genet.* 2015;61:373–82.
33. Vogt S, Rhiel A, Weber P, Ramzan R. Revisiting Kadenbach: electron flux rate through cytochrome c-oxidase determines the ATP-inhibitory effect and subsequent production of ROS. *Bioessays.* 2016;38:556–67.
34. Wang ZG, Ackerman SH. Identification of functional domains in Atp11p. Protein required for assembly of the mitochondrial F1-ATPase in yeast. *J Biol Chem.* 1996;271:4887–94.
35. Lefebvre-Legendre L, Salin B, Schaeffer J, Brèthes D, Dautant A, Ackerman SH, et al. Failure to assemble the alpha 3 beta 3 sub-complex of the ATP synthase leads to accumulation of the alpha and beta subunits within inclusion bodies and the loss of mitochondrial cristae in *Saccharomyces cerevisiae*. *J Biol Chem.* 2005;280:18386–92.
36. Netto LE, Antunes F. The roles of peroxiredoxin and thioredoxin in hydrogen peroxide sensing and in signal transduction. *Mol Cells.* 2016;39:65–71.
37. Yan L, Li M, Cao Y, Gao P, Cao Y, Wang Y, et al. The alternative oxidase of *Candida albicans* causes reduced fluconazole susceptibility. *J Antimicrob Chemother.* 2009;64:764–73.
38. Lu Y, Su C, Liu H. *Candida albicans* hyphal initiation and elongation. *Trends Microbiol.* 2014;22:707–14.
39. Kim S, Nguyen QB, Wolyniak MJ, Frechette G, Lehman CR, Fox BK, et al. Release of transcriptional repression through the HCR promoter region confers uniform expression of HWP1 on surfaces of *Candida albicans* germ tubes. *PLoS ONE.* 2018;13:e0192260.
40. Lee JH, Kim YG, Khadke SK, Yamano A, Watanabe A, Lee J. Inhibition of biofilm formation by *Candida albicans* and polymicrobial microorganisms by nepodin via hyphal-growth suppression. *ACS Infect Dis.* 2019;5:1177–87.
41. Lee JH, Kim YG, Choi P, Ham J, Park JG, Lee J. Antibiofilm and antivirulence activities of 6-gingerol and 6-shogaol against *Candida albicans* due to hyphal inhibition. *Front Cell Infect Microbiol.* 2018;8:299.

42. Cullen PJ, Edgerton M. Unmasking fungal pathogens by studying MAPK-dependent cell wall regulation in *Candida albicans*. *Virulence*. 2016;7:502–5.
43. Eggimann P, Garbino J, Pittet D. Management of *Candida* species infections in critically ill patients. *Lancet Infect Dis*. 2003;3:772–85.
44. Knafler HC, Smaczynska-de RII, Walker LA, Lee KK, Gow NAR, Ayscough KR. AP-2-dependent endocytic recycling of the chitin synthase Chs3 regulates polarized growth in *Candida albicans*. *mBio*. 2019;10:e02421–18.
45. Ugbogu EA, Wang K, Schweizer LM, Schweizer M. Metabolic gene products have evolved to interact with the cell wall integrity pathway in *Saccharomyces cerevisiae*. *FEMS Yeast Res*. 2016;16:fow092.
46. Wang O, Gellynck X, Verbeke W. Chinese consumers and European beer: associations between attribute importance, socio-demographics, and consumption. *Appetite*. 2017;108:416–24.
47. Orlean P. Architecture and biosynthesis of the *Saccharomyces cerevisiae* cell wall. *Genetics*. 2012;192:775–818.
48. Benedetti VP, Savi DC, Aluizio R, Adamoski D, Kava V, Galli-Terasawa LV, et al. ERG11 gene polymorphisms and susceptibility to fluconazole in *Candida* isolates from diabetic and kidney transplant patients. *Rev Soc Bras Med Trop*. 2019;52:e20180473.
49. Zorić N, Kosalec I, Tomić S, Bobnjarić I, Jug M, Vlainić T, et al. Membrane of *Candida albicans* as a target of berberine. *BMC Complement Alter Med*. 2017;17:268.
50. Guirao-Abad JP, Sánchez-Fresneda R, Román E, Pla J, Argüelles JC, Alonso-Monge R. The MAPK Hog1 mediates the response to amphotericin B in *Candida albicans*. *Fungal Genet Biol*. 2020;136:103302.
51. Wang YT, Liu JY, Shi C, Zhao JT, Xiang MJ. Knocking out ERG3 gene of *Candida albicans* and its effect on drug resistance. *J Shanghai Jiaotong Univ (Med Sci)*. 2020;40:163–70.